URSI GASS 2026, Kraków, Poland, 15 – 22 August 2026

GIRO-Based Ionospheric Electron Density Profile Model for HF Radio Propagation and Channel Modeling

Jarosław Wojtuń[(1)], Cezary Ziółkowski[(1)], Bogdan Uljasz[(1)] and Jan M. Kelner[(1)]
(1) Institute of Communications Systems, Faculty of Electronics, Military University of Technology, Warsaw, Poland

Abstract

This paper presents a compact, measurement-driven high-frequency (HF) ionospheric channel modeling approach intended for wideband waveform-level simulations. The model is parameterized using ionosonde-scaled characteristics from the Global Ionospheric Radio Observatory (GIRO) and reconstructs a time-varying F2-layer electron density profile using an analytic squared hyperbolic secant layer function. Based on this profile, the received signal is represented as a superposition of ordinary and extraordinary propagation components, whose complex reflection responses are computed using a closed-form expression consistent with the assumed profile. The frequency-dependent phase of the modal reflection responses yields mode-dependent effective delays, providing a physically grounded mechanism for delay spread. A representative case study based on GIRO data from the DB049 Dourbes station demonstrates that the proposed two-component model produces waveform distortion and inter-symbol interference (ISI) at the receiver input for symbol rates comparable to the modeled delay difference. The proposed framework provides a practical link between ionospheric sounding data and the generation of wideband HF channel responses, and it can be extended to include additional propagation mechanisms (e.g., E-layer contributions) in future work.

1. Introduction

High-frequency (HF) communication systems that rely on ionospheric propagation remain attractive for beyond-line-of-sight links, yet the ionosphere constitutes a strongly time-varying transmission medium. Temporal changes in the electron density distribution modify refraction and reflection conditions, which in turn affect the amplitude, phase, and effective propagation delay of the received signal. For modern HF waveforms with non-negligible bandwidth, these effects are not limited to slow fading: frequency-dependent delay and multipath components may introduce delay spread and, consequently, inter-symbol interference (ISI). Therefore, channel models intended for waveform design and performance assessment should enable a direct mapping from the ionospheric state to a wideband representation of the channel response.

A large body of HF channel modeling relies on stochastic, measurement-inspired formulations, with the Watterson model being a widely used reference for simulating ionospheric fading in HF links [1]. While such approaches are compact and convenient, they are typically employed to reproduce narrowband fading statistics and do not explicitly tie the channel response to the contemporaneous ionospheric state. For wideband HF systems, impulse-response–based modeling has been proposed to capture delay spread and waveform distortion, notably in the Vogler–Hofmeyer framework [2, 3, 4]. In parallel, routine ionosonde observations and global data services—such as the Global Ionospheric Radio Observatory (GIRO)—provide operational access to time-tagged ionospheric parameters that can drive measurement-informed channel models [5].

On the ionospheric side, analytic layer functions are commonly used to represent vertical electron density structure in a compact parametric form. In particular, $sech^2$-type (often referred to as Epstein-type) profiles have a long history in ionospheric modeling and are used in electron density profile reconstruction from ionogram-derived parameters as well as in reference ionosphere development [6, 7]. Such parameterizations are attractive because they provide a smooth peak and a physically plausible "thickness" control while remaining analytically tractable.

Motivated by these developments, this paper proposes a compact, measurement-driven HF channel modeling framework that links GIRO-derived F2-layer parameters to a dual-mode (ordinary/extraordinary) wideband channel representation. The F2-layer electron density is represented using a time-varying $sech^2$ profile whose parameters are obtained from scaled ionospheric characteristics. Based on this profile, the received signal is modeled as a superposition of the ordinary (O) and extraordinary (X) components, each described by a frequency- and time-dependent reflection response, amplitude, phase, and effective delay. This dual-mode representation provides a physically motivated mechanism for delay spread and enables straightforward generation of a wideband channel response suitable for baseband waveform simulations, where ISI can be observed directly at the receiver (Rx) input.

The remainder of the paper is organized as follows. Section 2 describes the GIRO data products used in this study and the adopted parameterization of the electron density profile. Section 3 presents the proposed dual-mode HF channel model and outlines the procedure for obtaining its time-varying parameters. Section 4 provides a representative case study and example results illustrating waveform distortion and ISI, and Section 5 concludes the

paper and outlines directions for an extended journal version.

2. GIRO Data and F2-Layer Electron Density Profile

This work uses ionosonde observations distributed through GIRO [8]. GIRO provides access to historical and near-real-time ionograms together with scaled ionospheric characteristics derived from routine sounding. In this paper we use GIRO Digital Ionogram DataBase (DIDBase) scaled parameters (nominal cadence of approximately 5 min) for the selected Digisonde station DB049 Dourbes. The following parameters are used to parameterize the F2 layer: the critical frequency $f_{oF2}(t)$, the peak height $h_{mF2}(t)$, and the half-thickness parameter $y_{F2}(t)$.

GIRO time series may contain missing samples for some parameters. To obtain continuous model inputs required by waveform-level simulations, missing values are filled by linear interpolation in time. The resulting parameter sequences are then resampled on a uniform simulation grid with a 1-s step, which provides a convenient numerical time base for time-varying channel updates. This resampling does not increase the intrinsic measurement time resolution of the ionosonde data; it only defines the update rate used by the simulator.

The time-varying F2-layer electron density profile is represented by a compact $sech^2$ -type analytic layer function [9],

$$N_e(z,t) = N_m(t) sech^2\left(\frac{z - h_{mF2}(t)}{a(t)}\right), \quad (1)$$

where $N_m(t)$ is the peak electron density, $h_{mF2}(t)$ is the peak height, and $a(t)$ controls the layer thickness. Here z, $h_{mF2}(t)$, and $a(t)$ are expressed in km, while N_e is expressed in m^{-3}. GIRO provides $y_{F2}(t)$ as the F2-layer half-thickness derived under a parabolic-layer assumption. In this work it is used as an effective thickness measure and mapped to the $sech^2$ scale parameter via $a(t) = 2y_{F2}(t)$. The peak density is obtained from the critical frequency via the plasma-frequency relation at the profile maximum [10],

$$N_m(t) = \left(2\pi f_{oF2}(t)\right)^2 \frac{\varepsilon_0 m_e}{e^2} \quad (2)$$

where e and m_e are the electron charge and mass, respectively, and ε_0 is the vacuum permittivity.

In this conference paper, we restrict the ionospheric description to the F2 layer to keep the model compact; incorporation of an additional E-layer component is left for the extended journal version.

Fig. 1 shows example F2-layer electron density profiles reconstructed from GIRO-scaled parameters for a representative midday interval at DB049 Dourbes. The set of curves illustrates the temporal variability of both the peak density and the effective layer thickness, which directly impacts frequency-dependent reflection and effective delay in the proposed HF channel model (Section 3).

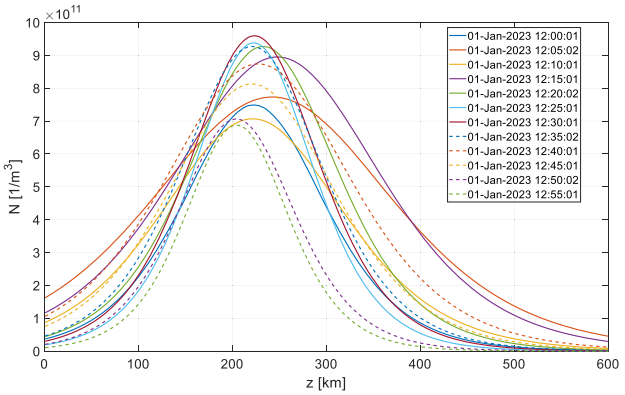


Figure 1. F2-layer electron density profiles $\boldsymbol{N_e(z,t)}$ reconstructed from GIRO scaled parameters (DB049 Dourbes), example midday interval.

3. Proposed HF Channel Model

In this paper, the ionospheric HF channel is modeled as a time-varying, frequency-dependent system driven by the reconstructed F2-layer electron density profile (Section 2). We assume that, for the considered link geometry and operating conditions, the useful received signal is dominated by two propagation components associated with the ordinary and extraordinary rays. The resulting signal at the Rx input is described as the following linear superposition:

$$s(f,t) = R_o(f,t)\cdot A_o(t) e^{j\left(2\pi f(t-\tau_o(t))-\varphi_o(t)\right)} + R_e(f,t)\cdot A_e(t) e^{j\left(2\pi f(t-\tau_e(t))-\varphi_e(t)\right)}, \quad (3)$$

where $R_o(f,t)$ and $R_e(f,t)$ are the complex reflection coefficients (magnitude and phase) for the ordinary and extraordinary components, $A_o(t)$ and $A_e(t)$ are amplitude weights, $\tau_o(t)$ and $\tau_e(t)$ are effective delays, and $\varphi_o(t)$ and $\varphi_e(t)$ are time-varying phases. The key wideband impairment mechanism is the delay difference

$$\Delta\tau(t) = \tau_o(t) - \tau_e(t), \quad (4)$$

which may produce delay spread and ISI when $\Delta\tau(t)$ becomes comparable to the symbol interval.

The core element of the proposed model is the reflection coefficient $R(f,t)$, which maps the ionospheric vertical structure onto the received signal. Assuming the F2-layer electron density profile in the $sech^2$ form (Section 2), the complex reflection coefficient for a plane wave of frequency f incident at angle θ can be expressed in a closed form involving Gamma functions [11]:

$$R(f,t) = -\frac{\Gamma\left(1-i\frac{2\pi f a\cos(\theta)}{c}\right)\Gamma\left(i\frac{2\pi f a\cos(\theta)}{c}+\frac{1}{2}+i\delta\right)\Gamma\left(i\frac{2\pi f a\cos(\theta)}{c}+\frac{1}{2}-i\delta\right)}{\Gamma\left(1+i\frac{2\pi f a\cos(\theta)}{c}\right)\Gamma\left(\frac{1}{2}+i\delta\right)\Gamma\left(\frac{1}{2}-i\delta\right)} exp\left\{-i\frac{2\pi f a\cos(\theta)}{c}(z_m - z)\right\}, \quad (5)$$

where $\Gamma(\cdot)$ denotes the Gamma function, c is the speed of light, $a(t)$ is the layer thickness parameter, and $z_m(t)$ is the altitude of maximum electron density (in this paper $z_m(t) = h_{mF2}(t)$). The parameter $\delta(t)$ is defined as:

$$\delta(t) = \frac{1}{2}\sqrt{\left(\frac{4\pi f_0(t) a(t)}{c}\right)^2 - 1}, \quad (6)$$

where $f_0(t)$ is the plasma frequency at the profile maximum (i.e., corresponding to the peak density $N_m(t)$).

$$f_0^2(t) = \frac{e^2 N_m(t)}{4\pi^2 \varepsilon_0 m_e}, \quad (7)$$

The reflection coefficient depends on the incidence/reflection angle θ, which is determined from the propagation geometry and the apparent reflection height. For each component, we compute mode-dependent apparent heights $h_o(f,t)$ and $h_e(f,t)$, and then approximate the corresponding angles using a simple geometric relation:

$$\theta_o(f,t) = \arctan\left(\frac{0.5d}{h_o(f,t)}\right), \quad (8a)$$

$$\theta_e(f,t) = \arctan\left(\frac{0.5d}{h_e(f,t)}\right), \quad (8b)$$

where d is the distance between the transmitter (Tx) and Rx. This approximation keeps the model computationally light while enabling frequency- and time-dependent reflection conditions.

The complex reflection coefficients contribute both magnitude and phase. In the adopted notation, the phase of each component is decomposed into an effective delay term and a residual phase term:

$$\arg\{R_o(f,t)\} = 2\pi f\, \tau_o(t) + \varphi_o(t), \quad (9a)$$

$$\arg\{R_e(f,t)\} = 2\pi f\, \tau_e(t) + \varphi_e(t), \quad (9b)$$

In practice, $\tau_o(t)$ and $\tau_e(t)$ can be estimated over the considered signal bandwidth by unwrapping the phase of $R_o(f,t)$, $R_e(f,t)$ and fitting a linear phase slope versus frequency.

At each simulation time step t (1 s grid), the model is updated as follows:

1. read and interpolate GIRO data $f_{oF2}(t)$, $h_{mF2}(t)$, $y_{F2}(t)$ and compute $N_m(t)$ and $a(t)$;
2. determine the mode-dependent apparent heights $h_o(f,t)$, $h_e(f,t)$ and angles $\theta_o(f,t)$, $\theta_e(f,t)$;
3. compute $R_o(f,t)$ and $R_e(f,t)$ using (5)–(7) and θ_o, θ_e;
4. estimate $\tau_o(t), \tau_e(t)$ and $\varphi_o(t), \varphi_e(t)$ from (9);
5. synthesize $s(f,t)$ using (3).

4. Scenario and Results

This section presents example results generated with the proposed GIRO-driven HF channel model. The considered path is defined between two cities in Poland – Rzeszów (Tx: 50.04119° N, 21.99912° E) and Szczecin (Rx: 53.42854° N, 14.55281° E), with a ground distance of approximately 635 km. GIRO DIDBase scaled parameters from the DB049 Dourbes Digisonde are used to reconstruct the time-varying F2-layer electron density profile (Section 2). Example results are shown for 01 Jan 2023 over the 12:00–12:55 universal time coordinate (UTC) interval. The model is updated on the uniform time grid used in the processed GIRO series. The Earth's magnetic field required for the ordinary/extraordinary mode separation is obtained from the world magnetic model (WMM) evaluated at the midpoint of the Tx–Rx path.

Fig. 2 shows the time evolution of the mode delay difference $\Delta\tau(t)$ between the ordinary and extraordinary components for three carrier frequencies (f = 3, 5, and 7 MHz). The results demonstrate that $\Delta\tau(t)$ is both time-varying and frequency-dependent, which is consistent with the wideband nature of the proposed model: temporal changes in the GIRO-reconstructed F2-layer profile translate into changes of the effective modal delays and their separation. For most of the analyzed interval, $\Delta\tau(t)$ remains within a few milliseconds ($|\Delta\tau(t)| < 5ms$), while occasional short-lived excursions are observed. Such excursions indicate time periods when the propagation conditions yield a larger separation between the ordinary and extraordinary contributions.

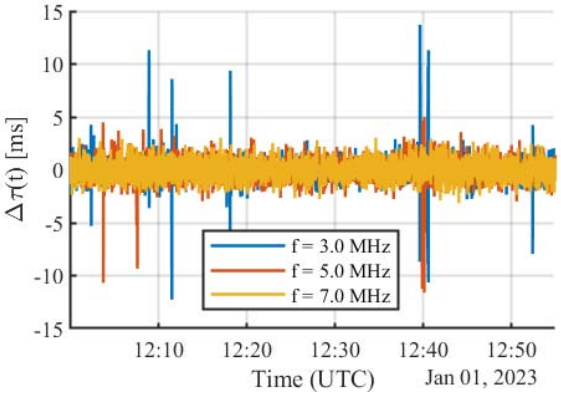


Figure 2. Ordinary/extraordinary mode delay difference for the Szczecin – Rzeszów HF link on 01 Jan 2023, 12:00–12:55 UTC, based on GIRO DB049 Dourbes inputs.

From a digital communications perspective, the mode delay difference $\Delta\tau(t)$ is an immediate indicator of potential waveform distortion. When the symbol interval becomes comparable to the instantaneous O/X delay separation, the superposition of the ordinary and extraordinary components produces symbol overlap and ISI. This effect is illustrated in Fig. 3 using binary phase shift keying (BPSK) at a fixed carrier frequency $f = 5$ MHz for a representative ionospheric state with $\Delta\tau = -11.5$ ms. As the bit rate increases from 600 bps to 1200 bps and 2400 bps, the eye progressively closes, confirming the expected increase of ISI severity with decreasing symbol duration.

5. Conclusions

This paper proposed a compact, measurement-driven approach to HF ionospheric channel modeling based on GIRO ionosonde observations. The F2-layer electron density profile is reconstructed from scaled GIRO parameters and represented with a $sech^2$-type analytic function, enabling time-varying channel parameter updates. Building on this profile, the received signal is modeled as a superposition of ordinary and extraordinary propagation components with frequency-dependent reflection responses, resulting in mode-dependent effective delays.

Example results for the Szczecin–Rzeszów HF link demonstrate that the ordinary/extraordinary delay difference $\Delta\tau(t)$ varies over time and depends on the carrier frequency (Fig. 2). This behavior indicates a physically motivated mechanism for wideband distortion and potential ISI when the symbol interval becomes comparable to the instantaneous mode delay difference.

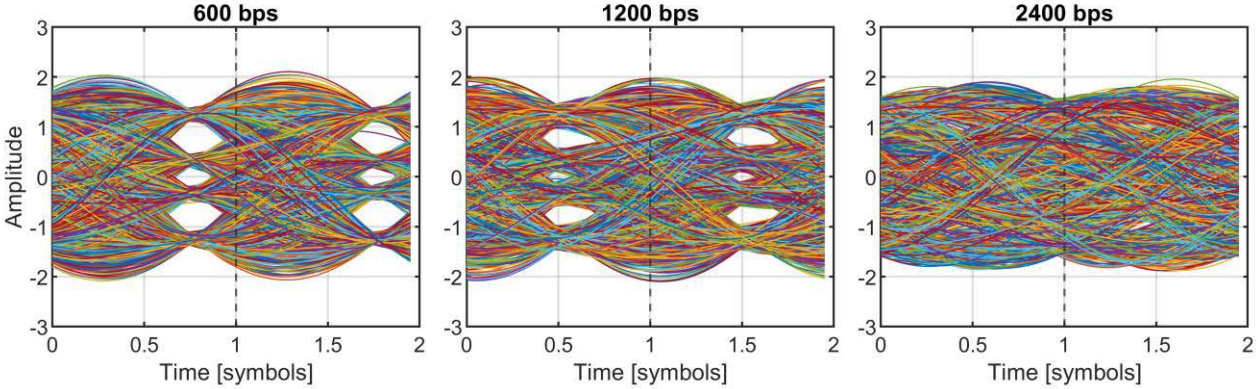


Figure 3. Eye diagrams for $\boldsymbol{f = 5}$ MHz at a representative time instant with $\boldsymbol{\Delta\tau = -11.5}$ ms (Szczecin – Rzeszów HF link, 01 Jan 2023, 12:40:07 UTC), shown for BPSK at 600, 1200, and 2400 bps (left to right).

Future work will extend the conference version in several directions: (i) incorporation of additional propagation mechanisms, including an E-layer component and more general multipath structures; (ii) broader validation across different days, seasons, and GIRO stations; (iii) inclusion of realistic background noise conditions following Recommendation ITU-R P.372 [12]; and (iv) benchmarking against established HF channel models, including the Waterson model and the Vogler–Hofmeyr model.

6. Acknowledgements

This work was supported by the Military University of Technology under research project no. UGB 531-000128-W300-22/2026 on *"Analysis of the possibility of using modern technologies in communication systems and electronic warfare"*.

References

[1] C.C. Watterson, J.R. Juroshek, and W.D. Bensema, "Experimental confirmation of an HF channel model," *IEEE Transactions on Communication Technology*, vol. 18, no. 6, pp. 792–803, Dec. 1970, doi: 10.1109/TCOM.1970.1090438.

[2] L.E. Vogler, J.A. Hoffmeyer, *A new approach to HF channel modeling and simulation, Part I: Deterministic model*, NTIA Report 88–240, 1988.

[3] L.E. Vogler, J.A. Hoffmeyer, *A new approach to HF channel modeling and simulation, Part II: Stochastic model*, NTIA Report 90–255, 1990.

[4] L.E. Vogler, J.A. Hoffmeyer, *A new approach to HF channel modeling and simulation, Part III: Transfer function*, NTIA Report 93–284, 1992.

[5] B.W. Reinisch , I.A. Galkin, "Global Ionospheric Radio Observatory (GIRO)," *Earth, Planets and Space*, vol. 63, pp. 377–381, Jun. 2011, doi: 10.5047/eps.2011.03.001.

[6] W. Lisiecki, „Propagacja fal radiowych," Wydawnictwo Komunikacji i Łączności, 1962 Warszawa.

[7] B. Uljasz, C. Ziółkowski, „Comparative analysis of ionosphere chargé density profile models used for signal prediction in HF channels," *Telecommunications Review, Telecommunications News*, vol. 96, no. 4, pp. 301–304, Sep. 2023, doi: 10.15199/59.2023.4.67.

[8] https://giro.uml.edu, Global Ionosphere Radio Observatory (GIRO), date: 2026.02.06.

[9] P.S. Cannon, "Extreme space weather—A report published by the UK Royal Academy of Engineering," *Space Weather*, vol. 11, no. 4, pp. 138–139, Apr. 2013, doi:10.1002/swe.20032.

[10] C.R. Mannix, D.P. Belcher, P.S. Cannon, and M.J. Angling, "Using GNSS signals as a proxy for SAR signals: Correcting ionospheric defocusing," *Radio Science*, vol. 51, no. 2, pp. 60–70, Feb. 2016, doi: 10.1002/2015RS005822.

[11] G.H. Price, "The characteristics of impulses reflected from a sech^2electron-density profile and bandpass filtered," Proceedings of the IEEE, vol. 56, no. 8, pp. 1341–1349, Aug. 1968, doi: 10.1109/PROC.1968.6575.

[12] Recommendation ITU-R P.372-17, P Series Radiowave propagation: Radio noise, ITU, 2024 Genewa.